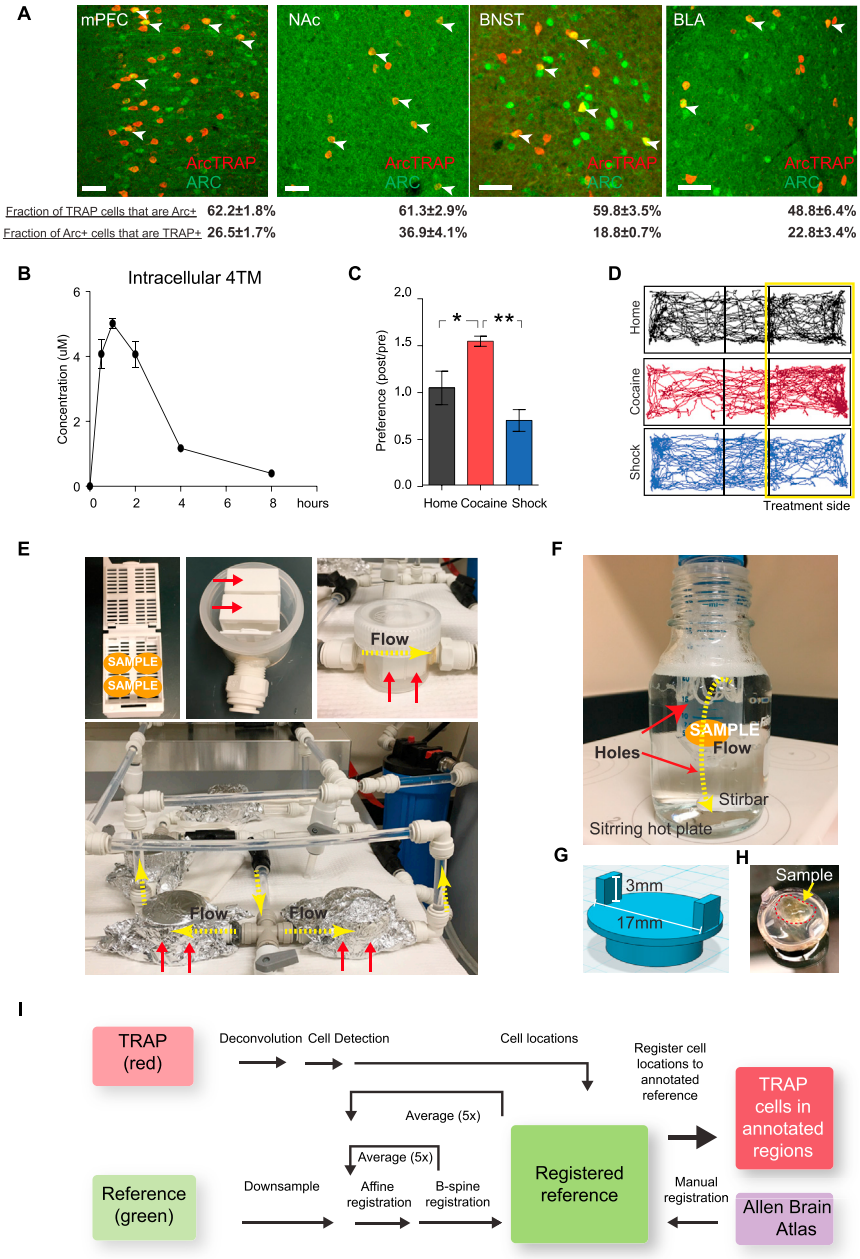

Figure S1. Behavioral Cohort-Scale Brain-wide Activity Mapping by CLARITY, Related to Figure 1

(A) Representative images and quantification (mean ± SEM, n = 4 mice per group) of colabeling between ArcTRAP and Arc immunostaining in indicated regions. Arrowheads indicate double-positive cells. Numbers in top row: fraction of ArcTRAPed cells that are Arc+; Bottom row: fraction of Arc+ cells that are ArcTRAPed. Note that the labeling by ArcTRAP is more stringent than Arc immunostaining (fewer TRAP+ cells than Arc+ cells overall). Scale bar: 50 μm.

(B) Pharmacokinetics of 4TM in mouse brain after a single intraperitoneal injection (10mg/kg); n = 5 per time point.

(C) Cocaine dosing (15mg/kg) and a series of foot shocks (0.5mA/2 s) lead to place preference and aversion, respectively. An independent cohort of mice was used to validate the stimuli used in the study as appetitive (cocaine) and aversive (shock) using a 3-chamber place preference test. After two days of indicated exposure, fold-change in preference for the side where cocaine or shock was given was quantified. n = 5 per group, *p < 0.05, **p < 0.01, unpaired t test. Error bars, mean ± SEM.

(D) Representative movement tracking data.

(E) Setup of parallel flow-assisted clearing. Up to 4 mouse brains can be inserted into a tissue cassette (30x40x12mm). Two cassettes (indicated by red arrows) are inserted into a chamber constructed with an inlet and outlet for buffer exchange. To scale up clearing, multiple chambers (each containing up to 8 brains) can be connected in parallel to a temperature-controlled circulator (calibrated so that the temperature in the sample chamber is kept at 40°C).

(F) Alternative flow-assisted clearing setup without using a circulator. A 50ml conical tube (with small holes drilled in the middle and on the bottom, as indicated by red arrows) can be inserted into a 250ml glass bottle filled with clearing buffer. Each tube fits 3-4 mouse brains. Unidirectional flow (yellow line) is created by using

(legend continued on next page)

a magnetic stir bar and a stirring hot plate to accelerate the clearing. Upon first use, the temperature of the hot plate needs to be set properly so that the buffer temperature is maintained at desired level inside the conical tube. The speed of the stirring should also be set properly so that proper flow is being generated without damaging the sample.
(G and H) Schematic and picture of the adaptor used for mounting brains onto the ultramicroscope (Lavision Biotec).
(I) Data processing pipeline for image registration, cell detection, annotation and quantification.

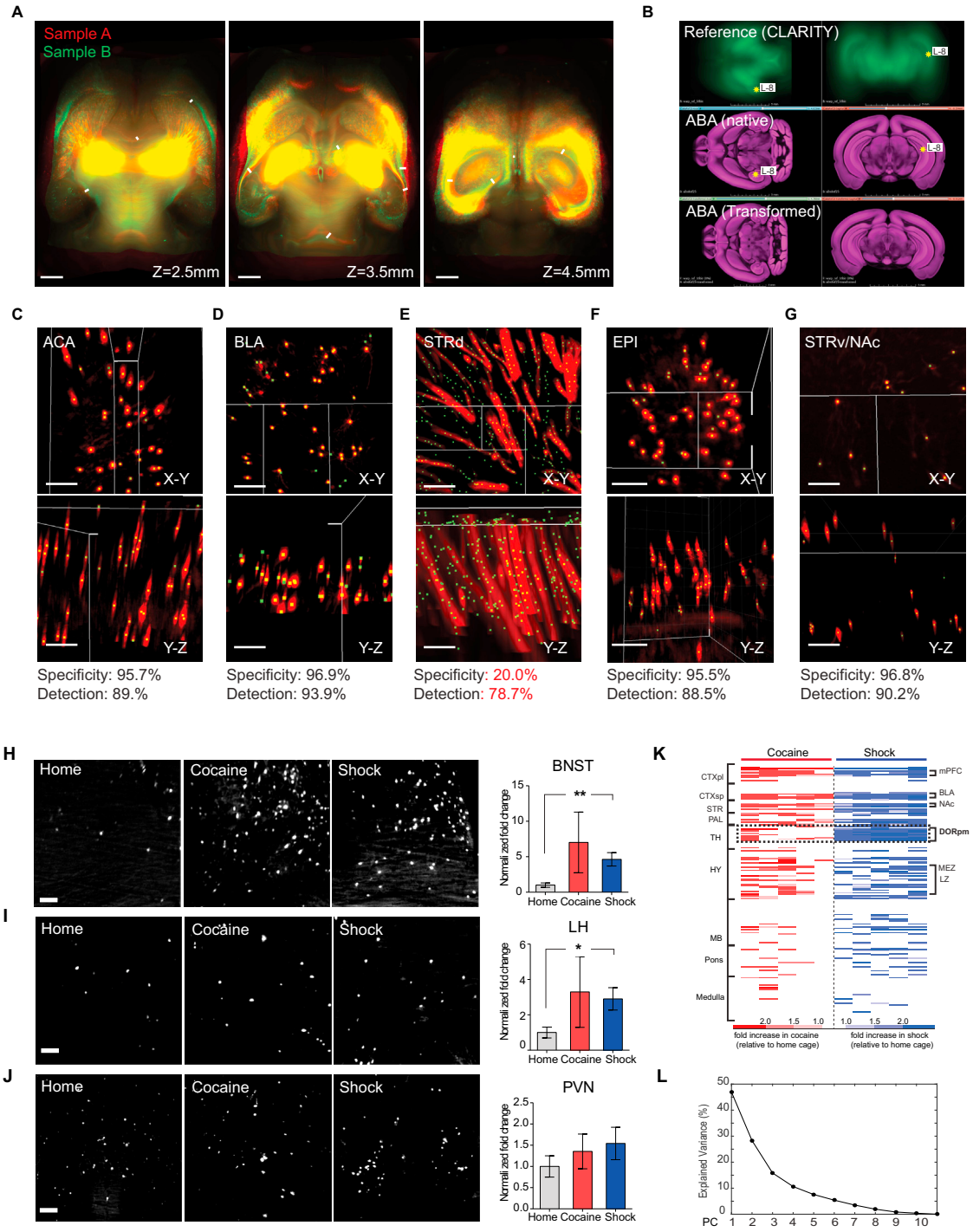

Figure S2. Cocaine and Shock Recruit Overlapping Brain Regions, Related to Figure 2

(A) Representative images illustrating alignment between individual brains after registration. TRAP signal from two individuals (one shown as red, the other as green) overlaid to show alignment. White bars indicate small remaining misaligned boundaries due to combined sources of structural variation and alignment error (~200μm). Scale bar: 500 μm.

(B) Representative images illustrating the manual ABA registration using 3D-Slicer. A total of 30 landmarks (showing one (#8) here) were manually placed in the CLARITY reference (top) and the ABA reference (middle). The program calculated the transform (using thin plate registration) and output the transformed ABA image (bottom).

(C–G) Representative images illustrating the automatic 3D cell detection in various brain regions. Top: cell detection in x-y plane; Bottom: cell detection in y-z plane. ACA: anterior cingulate cortex; BLA: basolateral amygdala; STRd: dorsal striatum; EPI: epithalamus; STRv/NAc: ventral striatum/nucleus accumbens.

(legend continued on next page)

Note that cell detection failed in STRd as the program could not distinguish fiber bundles from cell bodies. Therefore the STRd was excluded from all subsequent analysis. For quantifying detection accuracy, in each region, the specificity is defined by the percent of cells correctly detected (True positive / (True positive +False positive)) and detection is defined by percent of ground-truth cells detected (True positive/ (True positive + False negative)). Manually identified cells are used as "ground truth." Numbers represent means from three independent counts. Scale bar: 100 μm.

(H–J) TRAP cells in BNST, LH and PVN. Left: representative images taken at the center of the indicated regions (maximum projection of 100 μm volume). Scale bar: 100μm. Right: fold-change in TRAP cell numbers (normalized to home cage). n = 5 per group, *$p < 0.05$, unpaired t test. Error bars, mean ± SEM.

(K) Heat map showing cocaine- and shock- activated brain regions. Each column represents an individual mouse. Each row represents an individual brain region (~200 regions in total). Increase in TRAP cell counts in each region was color-coded as fold changes (red: increase cell counts in cocaine group; blue: increase cell counts in shock group; all normalized to home cage controls). Cocaine or shock activated areas were summarized as clusters of proximal regions. CTXpl/sp: cortical plate/subplate, SRT: striatum, PAL: pallidum, TH: thalamus, HY: hypothalamus, MB: midbrain. DORpm: polymodal association cortex-related dorsal thalamus. MEZ: Hypothalamic medial zone, LZ: Hypothalamic lateral zone.

(L) Percentage of total variance explained by each principal component in the PCA (Supplemental Experimental Procedures).

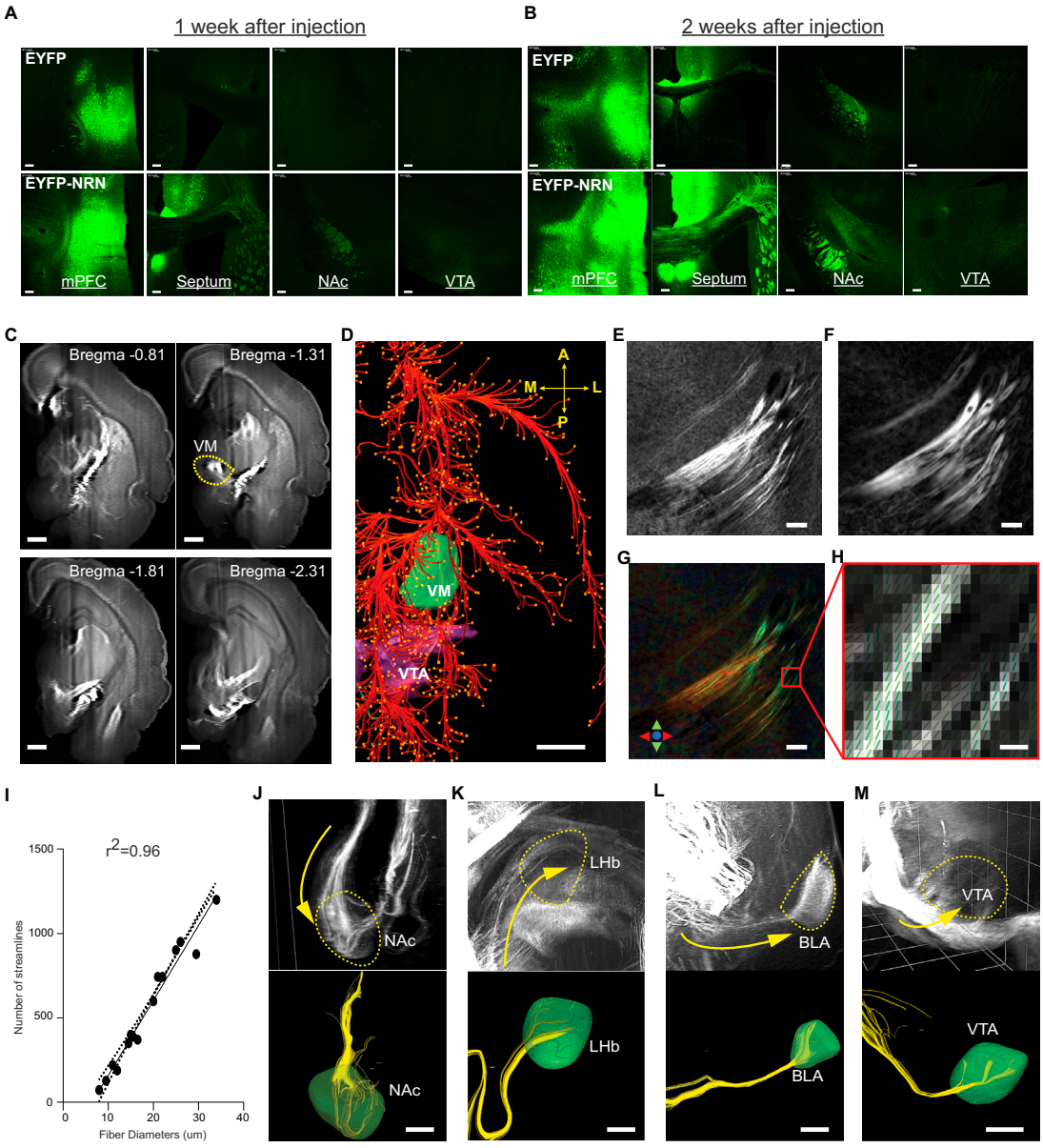

Figure S3. CLARITY Enables Brain-wide Projection Mapping, Related to Figure 3

(A and B) Representative images (n = 4 mice per group) showing side-by-side comparisons between EYFP and EYFP-NRN expression in downstream regions after a single mPFC injection (both under a CaMKIIα promoter). Note that EYFP-NRN travels faster than EYFP alone. Scale bar: 100 μm.

(C) 2D coronal sections (50μm max-projection) at the indicated locations (relative to bregma). Scale bar: 500 μm.

(D) A snapshot of putative mPFC to VM (ventral medial thalamus, highlight in green) projection paths (shown as red streamlines) from the Allen Brain mouse connectivity atlas (http://connectivity.brain-map.org/). Scale bar: 1mm.

(E–H) Representative intermediate steps of reconstructing axonal projection to streamlines using structural tensor based CLARITY tractography (Supplemental Experimental Procedures). (E) Raw CLARITY image, showing outgoing mPFC projections (EYFP). (F) Image intensity gradient amplitude, computed by convolving the 3-dimensional CLARITY image volume with three 3-dimensional 1st order derivative of Gaussian functions (σdog = 1 voxel/6 μm) along each of the x, y and z axes. (G) Color-coded principal fiber orientations (A-P: red; D-V, green; L-M, blue), estimated as the tertiary eigenvectors of computed structure tensors (σd = 1 voxel/6 μm, σdog = 1 voxel/6 μm). For better visualization, the color brightness was weighted by the raw CLARITY image intensity. Scale bars: 100 μm. (H) A zoomed-in region of (E) showing the principal fiber orientations as color-coded vector fields overlaid on raw CLARITY image. The vectors are color-coded for their orientation. Scale bar: 6μm.

(I) Correlation between the diameter of each axonal bundle and the number of streamlines representing that specific bundle. The diameter was determined at the cross-sections of each bundle. The numbers of passing streamlines are also measured at the same cross-sections. n = 15, Pearson correlation, $r^2 = 0.96$, $p < 0.0001$.

(J–M) Representative reconstructions of axonal projections (outgoing projections from mPFC) in various target regions. Top row: CLARITY images; bottom row: reconstructed streamlines ending in the indicated 3D regions.

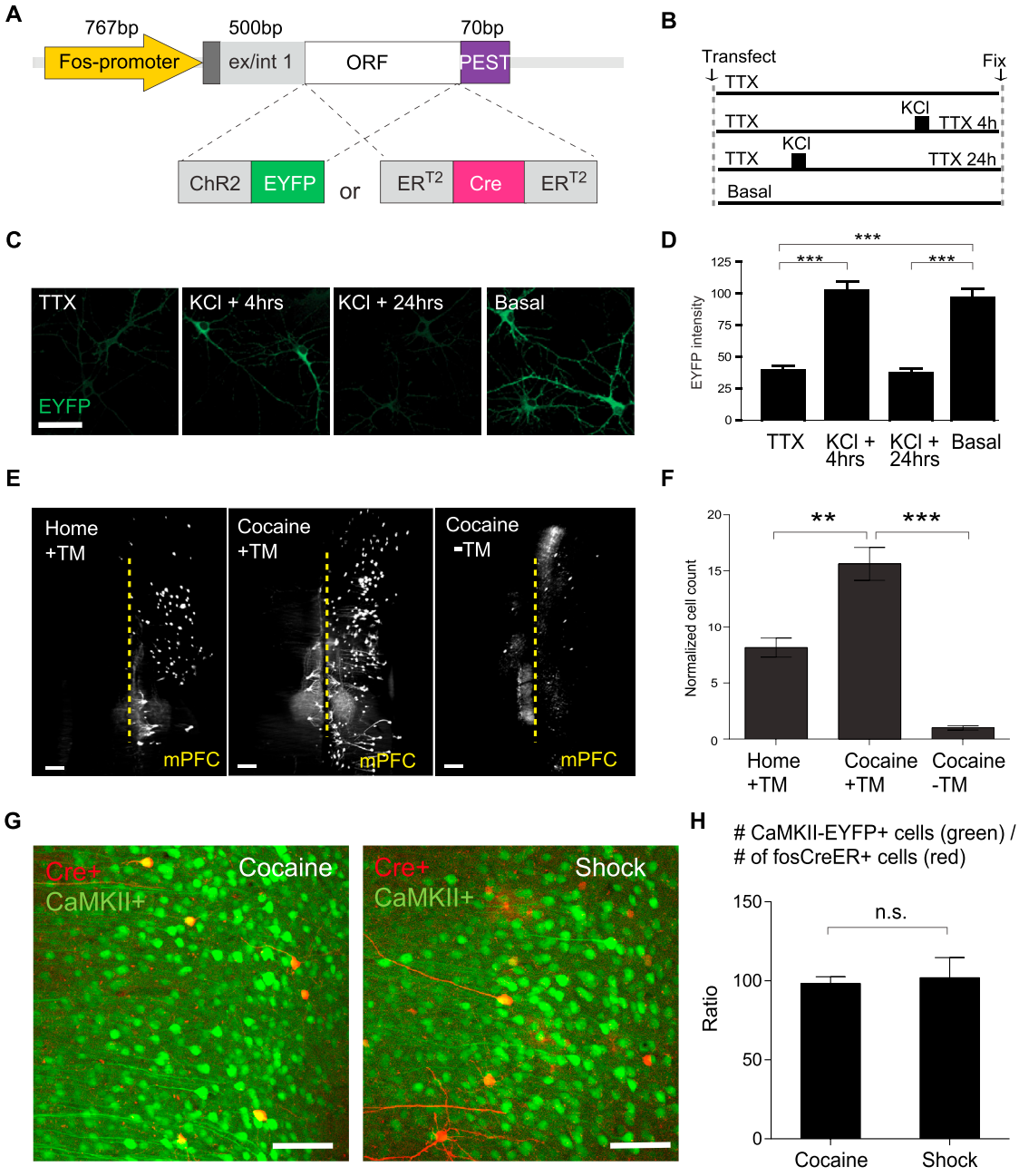

Figure S4. Validation of Activity-Dependent Constructs, Related to Figure 4

(A) Construction strategy. An expression cassette was inserted immediately after intron 1 of the c-*fos* gene. Either ChR2-EFYP (cFos-ChR2-EYFP, termed fosCh) or ER^{T2}-Cre-ER^{T2} fusion was inserted, followed by a 70bp PEST sequence to promote construct degradation (to further enhance specificity).

(B) Schematic to illustrate treatment of cultured hippocampal neurons following transfection of c-Fos-ChR2-EYFP. Neurons were electrically silenced with TTX, APV and NBQX; fosCh expression was compared to expression levels in "basal" (spontaneously synaptically active, but not otherwise stimulated or silenced) cultures. Following a 30 min depolarizing stimulus (60 mM KCl) the TTX/APV/NBQX solution was replaced and groups were fixed at the indicated time points.

(C) Representative images showing fosCh expression of cultured hippocampal neurons for each of the treatment groups. Scale bar: 25 μm.

(D) Quantification of mean pixel intensity of EYFP expression for conditions represented in c, n = 39-59 cells per group, $F_{3, 205} = 37.20$, ***$p < 0.001$, ANOVA followed by Tukey's multiple comparison test. (E-F) AAV-cFos- ER^{T2}-Cre-ER^{T2}-PEST was injected into the mPFC of Ai14 Cre-reporter mice. The mice were divided into three groups (n = 5 per group): home cage with 4TM, cocaine-injected with 4TM and cocaine-injected without 4TM.

(E) Representative images showing 4TM-dependent and activity-dependent labeling of mPFC neurons (tdTomato+), scale bar: 100 μm.

(F) Quantification tdTomato+ mPFC cells in three groups (normalized to the No-4TM group).

(G and H) Representative images and quantification showing CaMKIIα (green) and fosCreER (red) viruses target neurons at a constant ratio between two conditions. Scale bar: 50 μm. **$p < 0.01$, ***$p < 0.001$, unpaired t test. Error bars, mean ± SEM.

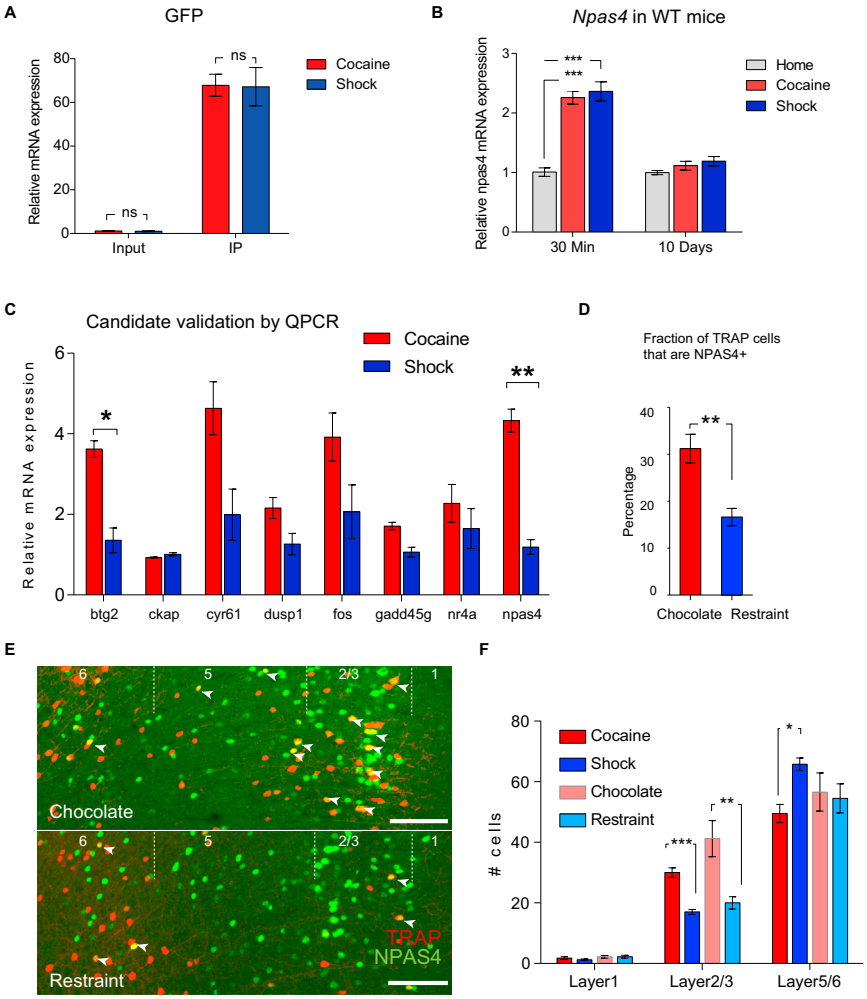

Figure S5. Positive Valence Experience Preferentially Activates the NPAS4+ Population in mPFC, Related to Figure 5

(A) Quantitative PCR analysis of GFP mRNA from the input and IP fraction of the cocaine- and shock-tagged mPFC population. Immunoprecipitation lead to 60- to 70-fold enrichment of GFP mRNA under both conditions (comparing Input to IP; Supplemental Experimental Procedures).

(B) Quantitative PCR analysis of mPFC Npas4 mRNA expression in the wild-type mice, 30 min and 10 days after the acute stimuli (cocaine or shock) exposure.

(C) Quantitative PCR validation of candidate genes (showing > 2.0 fold change, disregard p values, from cocaine IP versus shock IP (Figure 5B)). 1 of the 9 genes enriched in cocaine-cells was excluded (Gm6592, predicted gene); 2 of the 2 shock-enriched genes were excluded: ttr (transthyretin, undetectable by QPCR) and zfa (pseudogene). Out of the remaining eight genes, only Npas4 and Btg2 passed qPCR validation ($p < 0.05$).

(D and E) Quantification and representative images showing the overlap between TRAP+ (labeled by chocolate consumption and restraint; Supplemental Experimental Procedures) and NPAS4+ cells in the mPFC. Arrowheads indicate double positive cells. Scale bar: 100 μm.

(F) Layer distribution of TRAP cells with positive (cocaine or chocolate) experiences and negative (shock or restraint) experiences. n = 4-5 per group, ns, $p > 0.05$; *$p < 0.05$; **$p < 0.01$; ***$p < 0.001$; unpaired t test with Holm-Sidak correction. Error bars, mean ± SEM.

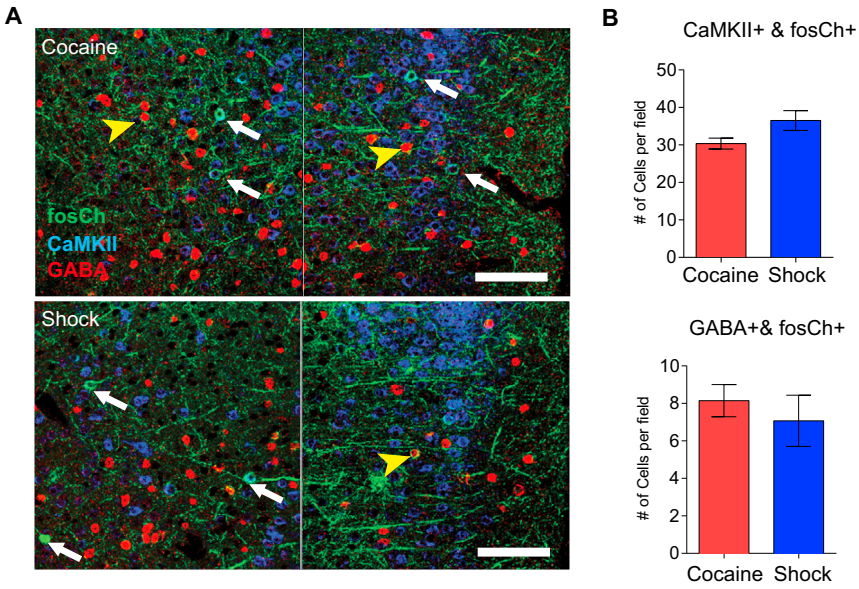

Figure S6. Use of fosCh for Targeting Cocaine- and Shock-Activated mPFC Populations, Related to Figure 6

(A) Representative confocal images showing fosCh expression in mPFC sections co-labeled with anti-GABA, and anti-CaMKIIα antibodies as indicated. White arrows indicate fosCh+/CaMKIIα+ neurons. Yellow arrowheads indicate fosCh+/GABAα+ neurons. Two 40X images were stitched together to visualize all cortical lamina. Scale bar = 100 μm.

(B) Quantification revealed no significant difference in the number of CaMKIIα-positive (left) and GABA-positive (right) fosCh cells for cocaine and shock groups. n = 10-14 mice per group. Error bars, mean ± SEM.

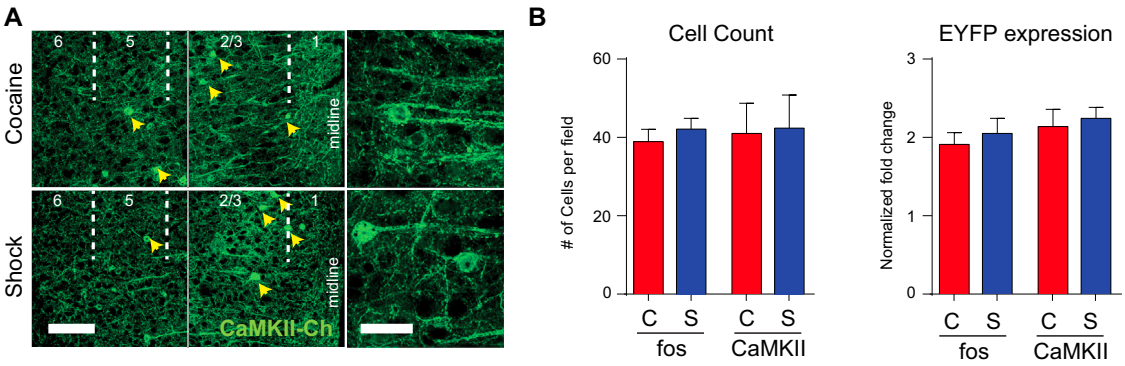

Figure S7. Use of CaMKIICh for Targeting Non-selective mPFC Populations, Related to Figure 7

(A) Representative images showing mPFC expression of CaMKIIα-ChR2 control conditions. Left, two 40X images were stitched together to visualize all cortical lamina. Scale bar = 100 μm. Right, high magnification images of individual CaMKIIα-ChR2 neurons. Scale bar = 25 μm.

(B) Quantification revealed no significant difference in the number of labeled cells (left) or level of EFYP expression (right) between CaMKIIα-ChR2 and fosCh conditions. n = 13 mice per group. Error bars, mean ± SEM.

Cell, Volume *165*

Supplemental Information

Wiring and Molecular Features of Prefrontal Ensembles Representing Distinct Experiences

Li Ye, William E. Allen, Kimberly R. Thompson, Qiyuan Tian, Brian Hsueh, Charu Ramakrishnan, Ai-Chi Wang, Joshua H. Jennings, Avishek Adhikari, Casey H. Halpern, Ilana B. Witten, Alison L. Barth, Liqun Luo, Jennifer A. McNab, and Karl Deisseroth

Supplemental Experimental Procedures

Constructs

The pAAV-fos-ChR2-EYFP (fosCh) plasmid was constructed by fusing the codon-optimized ChR2 (H134R) tagged with enhanced yellow fluorescent protein to a truncated c-fos gene sequence that included the 767 bp minimal promoter segment and the 500 bp intron 1 coding region containing key regulatory elements. A 70 bp PEST sequence was inserted at the C-terminal end to promote degradation and thereby prevent the membrane targeted ChR2-YFP from accumulating over time. The construct was cloned into an AAV backbone. The pAAV-fos-ER^{T2}-Cre- ER^{T2}-PEST plasmid was constructed by replacing the ChR2-EYFP in the fosCh plasmids with an ER^{T2}-Cre-ER^{T2} cassette (Kawashima et al., 2013). The pAAV-CaMKIIα-EYFP-NRN plasmid was constructed by replacing the 479 bp hGH polyA tail in pAAV-CaMKIIα-eYFP-WPRE-hGHpa (Tye et al., 2011) with a DNA fragment containing the 992 bp 3' UTR of Neuritin plus 215 bp bGH poly A flanked by AfeI and BstEI sites (NRN from the 3' UTR of the rat neuritin mRNA, (NM_053346.1)) (Akten et al., 2011).

Virus and injection

Adeno-associated viral (AAV) vectors were serotyped with AAV5 or AAV8 coat proteins and packaged by the University of North Carolina Vector Core and Stanford University Vector Core. Injections were made unilaterally into the PFC with final viral concentrations of AAV8-fos-ERT2-Cre-ERT2-PEST: $3x10^{12}$, AAV8-CaMKIIα-EYFP-NRN: $1.5x10^{12}$, AAV8-EF1α-DIO-EYFP-NRN: $5x10^{12}$, AAV5-fosCh-YFP: $2x10^{12}$, AAV5-CaMKIIα-YFP: $1.5x10^{11}$, all as genome copies per mL.

Stereotaxic surgery

6-7-week-old mice were anaesthetized with 1.5–3.0% isoflurane and placed in a stereotaxic apparatus (Kopf Instruments). Surgeries were performed under aseptic conditions. A scalpel was used to open an incision along the midline to expose the skull. After performing a craniotomy, viruses was injected into the mPFC using a 10 µl nanofil syringe (World Precision Instruments) at 0.1 µl min−1. The syringe was coupled to a 33 gauge beveled needle, and the bevel was placed to face the anterior side of the animal. The syringe was slowly retracted 20 min after the start of the infusion. A slow infusion rate followed by 10 min of waiting before retracting the syringe was crucial to restrict viral expression to the target area. Infusion coordinates were: anteroposterior, 1.9 mm; mediolateral, 0.35 mm; dorsoventral, 2.6 mm. Coordinates for the unilateral implantation of fiber optic cannulae (Doric Lenses 200 µm diameter) were: anteroposterior, 1.9 mm; mediolateral, 0.35 mm; dorsoventral, -2.4 mm. All coordinates relative to bregma.

ArcTRAP labeling

Male ArcTRAP (ArcCreER+/-, Ai14+/-) mice were used for study. 6-7 week old ArcTRAP mice were handled and injected with saline daily for at least 5 days prior to the experiment (including the home cage controls) to minimize the labeling due to handling and injections. The mice were 7-8 weeks old at the time of behavioral labeling. On experimental day 0, animals from both cocaine and shock groups were individually placed in a plastic chamber equipped with a grid floor connected to a shock generator, for 10 minutes to acclimatize the animals to the chamber (without receiving any actual shock or cocaine). On the following two days (experimental day 1 and day 2), animals were individually placed in the chamber for 10 minutes right after receiving 15 mg/kg intraperitoneal cocaine (cocaine group) or to receive 20 random foot shocks (2s, 0.5mA, 2 shocks per minute on average, shock group). The home cage control group remained in their home cage for the whole period. All the chambers were cleaned with 70% ethanol between trials. On experimental day 2, all mice received 5 mg/kg 4TM (IP injection) 3 hours after the behavioral challenge to enable TRAP labeling.

For ArcTRAP and Arc dual labeling: the mice were shocked (using the protocol above) in the presence of 5 mg/kg 4TM. The same animals were shocked again 96 hours after the first shock session and sacrificed 60 minutes later for Arc immunostaining. To verify that the resulting high level of overlap (~60%) in cells activated by different presentations of the same experience was not attributable to a population of constitutively active neurons in a particular field of view with activity unrelated to stimulus presentation, a shock-TRAPped animal was acutely injected with cocaine to label contrasting experiences (TRAP: shock; Arc staining: cocaine), which was found to result in low TRAP/Arc overlap in the mPFC (29.4±1.4%, as fraction of TRAP cells that were Arc+, or 14.0±2.4% as fraction of Arc+ cells that were TRAP+; mean± s.d., n=3 technical repeats from multiple fields of view). This finding was quantitatively replicated in a second animal (resulting 32.8±2.4% of TRAP cells that were Arc+ or

13.3±2.6% Arc+ cells that were TRAP+). These findings are also concordant with and supported by earlier work in the same mouse line (in the original TRAP paper; Guenthner et al, Neuron, 2013).

For labeling with a different set of positive/negative experiences: mice were individually housed one week before the experiments. On experimental day 1, a food pellet (1 gram mixture of milk chocolate and peanut butter) was given to the chocolate group for 1 hour to familiarize them with chocolate. The other group were restrained in rodent restrainer for 1 hour. On day 2, same chocolate pellets were given to the chocolate group and at least 0.5g was consumed within 1 hour. The restrain group were restrained again for 1 hour. Both groups received 5 mg/kg 4TM 3 hours after the beginning of the treatments to label the activated cells. All groups, including the home cage controls, received 4-hyroxytamoxifen injections at the same time of the day (2-3PM). The bedding of all cages was refreshed daily for 48 hours to prevent 4TM retake. All labeled mice were kept in their home cage for an additional 10 days to allow the full expression of tdTomato before perfusion.

Activity-dependent ribosome labeling

Male Arc-rTag mice were trained and labeled with 4TM with the same protocol used in ArcTRAP labeling. After labeling, the mice were returned and kept in their home cage for 14 days to allow full integration of tagged ribosomes.

Delivery of 4-hydroxytamoxifen

An aqueous formulation (instead of oil, which tends to give slower drug release) is designed to facilitate transient 4TM delivery (Ye et al., 2012). 10mg of 4TM (Sigma H6278) was first dissolved in 250 µl DMSO. This stock is first diluted in 5 ml of saline containing 2% Tween 80 and then diluted 1:1 again with saline. The final injectable solution contained: 1 mg/ml 4TM, 1% Tween 80 and 2.5% DMSO in saline. The pharmacokinetics of 4TM in mouse brain (using the above vehicle) was determined using a standard LS-MS method at Biomaterials and Advanced Drug Delivery Laboratory at Stanford. Briefly, 30 C57BL/6J mice were injected (IP) with 10 mg/kg 4TM at indicated time points (n=5 each time point) and n=5 mice injected with vehicle alone were used as blank control. Brains were collected after perfusion using 1X PBS at different time points and snap-frozen in liquid nitrogen before homogenized for Liquid Chromatography Mass Spectrometry (LC-MS) analysis.

CLARITY processing

The three key features of this new approach were: 1) accelerated clarification through parallelized flow-assisted clearing crucial for large cohorts (Figure S1D-G) independent of specialized equipment such as electrophoresis or perfusion chambers; 2) >90% cost reduction (also important for these large behavioral cohorts) using a new refractive index-matching process; and 3) optical properties such that the whole mouse brain can be imaged using a commercial light-sheet microscope under a single field of view (FOV) and as a single stack (~1200 steps across a ~6.6mm range) in less than 2 hours with single-cell resolution throughout the whole volume (this speed and simplicity is also critical for large behavioral cohorts; Figure 1C, D). Raw data files from each brain are ~12 GB in size and can be easily stored and directly analyzed on standard desktop workstations without the need for compression or stitching.

A hydrogel based on 1% acrylamide (1% acrylamide, 0.125% Bis, 4% PFA, 0.025% VA-044 initiator (w/v), in 1X PBS) was used for all CLARITY preparations. Mice were transcardially perfused with ice-cold 4% PFA. After perfusion, brains were post-fixed in 4% PFA overnight at 4°C and then transferred to 1% hydrogel for 48 hours to allow monomer diffusion. The samples were degassed and polymerized (4-5 hours at 37°C) in a 50ml tube. The brains were removed from hydrogel and washed with 200mM NaOH-Boric buffer (pH=8.5) containing 8% SDS for 6-12 hours to remove residual PFA and monomers. Brains could now be transferred to a flow-assisted clearing device using a temperature-control circulator or a simpler combination of 50ml tube and heated stirring plate (Figure S1D-E). 100mM Tris-Boric Buffer (pH=8.5) containing 8% SDS was used to accelerate the clearing (at 40°C). Note that Tris-containing buffer should only be used after PFA is completely washed out as Tris may potentially interact with PFA. With this setup, a whole mouse brain can be cleared in 12 days (with circulator, or 8 days for a hemisphere) or 16 days (with conical tube/stir bar). After clearing, the brain was washed in PBST (0.2% Triton-X100) for at least 24 hours at 37°C to remove residual SDS. Brains were incubated in a refractive index matching solution (RapidClear, RI=1.45, Sunjin lab, http://www.sunjinlab.com/) for 8 hours (up to 1 day) at 37°C and then 6-8 hours at room temperature. After the RC incubation, the brains were ready for imaging.

A 2-step TSA amplification strategy was used for immunostaining in thick CLARITY sections (such as the NPAS4 staining in Movie S1) to ensure homogeneous staining throughout the depth. 2mm sections were first stained with anti-NPAS4 antibody (1:3000, 6 days at 4°C in 0.3% PBST) and then stained with a secondary antibody conjugated with HRP (1:1000, 4 days at room temperature in 0.3% PBST). Samples were washed at least 24 hours at room temperature between steps. After 2nd antibody, samples were first incubated with TSA-Cy5 substrate (1:50, Perkin Elmer) or Alexa 647 Tyramide (1:50, Molecular Probes) in PBST containing 20% DMSO and 0.3% Triton-X100 (instead of the TSA amplification buffer or H_2O_2) at room temperature for 4 hours to allow efficient penetration of the substrate without reacting with HRP. Samples were then switched to TSA amplification buffer or 0.0015% H_2O_2 containing TSA-Cy5 substrate or Alexa 647 Tyramide (1:200) for additional 20 minute at room temperature to allow tyramide labeling. Samples were thoroughly washed for another 24 hours in 0.3% PBST at room temperature before mounting and imaging.

CLARITY imaging

Light-sheet imaging: Whole brain and hemisphere images were acquired with the Ultramicroscope II (Lavision Biotec). Samples were mounted to a custom 3D printed holder (Figure S1F-G) using RapidClear Mounting Gel (Sunjin lab). For whole brains (TRAP brains), the brain was mounted with the ventral side on top. For hemisphere, the cut surface (midline of the brain) was placed in touch with the holder and with the most lateral part on the top. Samples were securely mounted to the holder after mounting gel solidified (~5 minute at 4°C). Mounted samples were imaged inside an imaging chamber filled with 150ml of Rapidclear (reusable by periodical filtering). Samples were left in imaging chamber for 20-40min before imaging to allow the equilibrium of imaging liquid. Brains were imaged using a 2x/0.5NA objective at 0.6x zoom (whole brain, TRAP) or 0.8x zoom (hemisphere, CAPTURE). Multi-color imaging was enabled by applying filters setting to a supercontinuum white laser (NKT photonics). Samples were with two light sheets (NA=0.144) illuminating from both sides of the sample. Z-step was set to 5.16µm (at 0.6x zoom) or 4µm (at 0.8x zoom). Five horizontal focal points were set to each imaging plane for creating a homogeneous field of view.

Confocal imaging (Movie S1): Clarified tissues (2mm coronal sections) were incubated in Rapidclear CS for 1 day and mounted using a Wilco dish. The tissues were then imaged using an Olympus FV1200 system equipped with a 10x water-immersion objective (numerical aperture: 0.6; working distance: 3mm; step size, 3µm).

Image processing and visualization

All raw images were acquired as 16-bit TIFF files. The raw images were further processed by blind 3D deconvolution using AutoQuantX3 (Media Cybernetics). The parameters of the deconvolution were based on published methods using a similar light sheet microscope with a few modifications (Tainaka et al., 2014). Briefly, the modality was set to "Multi-photon fluorescence" 3D-blind deconvolution with 20 iterations. Noise was set to zero and using "unfiltered image" as "initial guess". In the expert settings, montage was turned on XY but off on Z, with 30-pixel overlap in XYZ. Other settings such as NA, spacing and magnitude were set based on the actual experiments. Either deconvolved or raw images can be 3D-rendered and visualized using Imaris (Bitplane, v8.1.2), for taking snapshot images and making movies.

Registration and quantification (TRAP analysis)

Briefly, after deconvolution, images of the TRAP brains were downsampled 4x, a subset were used to generate an average reference brain, individual samples were nonlinearly registered to that average reference, and then that registration was applied to the locations of individual cells to count cell numbers using an anatomical atlas in the reference space. Registration was performed on the reference (autofluorescence channel) using elastix(Klein et al., 2010).

Detailed procedures: To initialize the reference, 21 brains and their reflection across the midline axis of the image volume (total of 2*21=42 samples) were globally aligned to the Allen Brain Atlas Nissl-stained volume and then averaged. Each brain was then affine registered to the current average five times, and then resulting registered brains were again averaged to provide the input to the next iteration. Finally, all the brains were nonlinearly registered to the current reference (using an affine transformation as initialization), then averaged, for five iterations.

Each of the experimental samples was then nonlinearly registered to the average reference. Cell locations were detected in deconvolved images using Imaris (v8.1.2 Bitplane). The resulting nonlinear transformation for each brain was applied to every cell location found. Binary mask volumes were made for each brain region in the atlas

either manually drawn or from aligned Allen Brain Atlas (manually registered using 30 landmarks, using 3D-slicer http://www.slicer.org/) and indices from these mask volumes were used to compute the number of warped cell locations in each anatomical region. Of note, we excluded the regions where ArcTRAP is known to have strong non-tamoxifen dependent labeling (hippocampus, somatosensory and motor cortex)(Guenthner et al., 2013). Also, consistent with the original paper, AcrTRAP labeling was mainly in the forebrain; therefore, although we detected sparse signal/changes in the broader midbrain/hindbrain regions, the manual validation and analysis was focused on the forebrain. Principal component analysis was performed in MATLAB on the fold-change values relative to controls of all brain regions containing non-zero values.

Manually-defined brain regions: the 3D reference brain was digitally resliced into coronal sections with 100 µm spacing. Eight regions were drawn onto every coronal section with manually identified boundaries based on Allen Brain Atlas. The 2D contours were then used to generate a 3D surface using Imaris to quantify the cell numbers for each brain region.

Histology

Mice were deeply anaesthetized and transcardially perfused with ice-cold 4% paraformaldehyde (PFA) in PBS (pH 7.4). Brains were fixed overnight in 4% PFA and then equilibrated in 30% sucrose in PBS. 40 µm thick coronal sections were cut on a freezing microtome and stored in cryoprotectant at 4ºC until processed for immunostaining. Free-floating sections were washed in PBS and then incubated for 30 min in 0.3% Triton X-100 (Tx100) and 3% normal donkey serum (NDS). Slices were incubated overnight with 3% NDS and primary antibodies including: rabbit anti-GABA (Sigma A2052 1:200), mouse anti-CaMKIIα (Abcam ab22609 1:200), chicken anti-GFP (Abcam ab13970 1:500), Arc (SYSY 156003, 1: 4000) and rabbit anti-NPAS4 (a gift from Michael Greenberg, 1:3000). Sections were then washed and incubated with secondary antibodies (Jackson Labs 1:1000) conjugated to donkey anti-rabbit Cy5, anti-mouse Cy3 and anti-chicken FITC for 3 hrs at room temperature. All Arc and NPAS4 staining was performed using a TSA-plus-Cy5 amplification system (Perkin Elmer). Following a 20 min incubation with DAPI (1:50,000) sections were washed and mounted on microscope slides with PVA-DABCO. Confocal fluorescence images were acquired on a Leica TCS SP5 scanning laser microscope using a 40X/1.25NA oil immersion objective or a 10X/0.6NA water immersion objective. Serial stack images covering a depth of 20 µm (for fosCh experiments) or 40 µm (all other experiments) through multiple sections were analyzed by an experimenter blind to treatment condition. A 700 x 350 µm region of interest (ROI) centered in dorsal mPFC (manually defined based on DAPI staining) was used for cell counting. Average cell counts from five coronal slices (per mouse) were used as "# of cells per field" in all quantifications.

Ribosome profiling and molecular biology

Immunoaffinity purification of ribosome RNA from mPFC was carried out similarly to a protocol previously described(Sanz et al., 2009) with minor modifications. For preparation of anti-GFP-conjugated dynabeads, for each sample 50 µl protein G dynabeads (Life Technologies) was first washed with PBST and then incubated with 2 µl anti-GFP antibody (Abcam, ab290) in a total volume of 200 µl PBST. After incubating for at least 20 min at room temperature, the PBS-T was removed and the tissue lysates were immediately added to the beads, as described below. mPFC tissue was harvested using a 2mm-diameter tissue punch on freshly cut 2mm-thick coronal sections (cut using pre-chilled brain matrix). mPFC from 5 brains were pooled into one tube and then manually dounce-homogenized in 1 ml of IP buffer [50 mM Tris, pH 7.5; 12 mM MgCl2; 1%NP-40; 100 µg/ml cycloheximide (Sigma); 0.5 mM DTT; 100 mM KCl; 1x HALT protease inhibitor EDTA-free (Thermo); 1 mg/ml sodium heparin (Sigma); 0.2 units/µl RNasin (Promega)]. Following vortexing and centrifugation (12,000 x g for 10 min), 50 µl of the supernatant was taken as "input", and the remaining supernatant was incubated with the anti-GFP conjugated dynabeads for immunoprecipitation (IP fraction). After 2 h at 4°C, dynabeads were separated and washed twice with 1 ml high salt buffer [50 mM Tris, pH 7.5; 12 mM MgCl2; 1% NP-40; 100 µg/ml cycloheximide (Sigma); 0.5 mM DTT; 300 mM KCl]. Following the last wash, TRIzol (500 µl, Life Technologies) was immediately added to the beads (IP fraction). Another 500 µl TRIzol was added to the 50 µl input fraction collected earlier. RNA was purified using RNeasy Micro Kit (Qiagen) according to the manufacturer's instructions. RNA samples (all at 100ng per sample) were processed at the Stanford Protein and Nucleic Acid Biotechnology Facility by one-cycle target preparation, labeling and hybridization to Mouse Gene 2.0 ST Array (Affymetrix), according to the manufacturer's protocol and analyzed by Affymetrix Transcriptiome Analysis Console. The accession number for the microarray data reported in this paper is GEO: GSE76851. For qPCR analysis, RNA was reverse transcribed using the ABI high

capacity cDNA synthesis kit and used in quantitative PCR reactions containing SYBR-green fluorescent dye (ABI). Relative expression of mRNAs was determined after normalization with TBP levels using the ΔΔCt method.

Reconstruction and analysis of projections

Tractography methodology akin to what is used for diffusion MRI was used to reconstruct 3D models of fiber bundle trajectories based on the CLARITY data. The tractography algorithm (Mori et al., 1999) propagates streamlines from a "seed" region through a vector field of voxel-wise principal fiber orientations and terminates if a streamline makes a sharp turn (angles larger than a prescribed threshold α_{thresh}) or ventures outside of the masked region. The "seed" region (injection site) is manually identified based on the actual boundaries of maximal CaMKIIα-EYFP expression (green signal), which for the experiments presented in Fig. 4 were measured to span: anteroposterior, 2.0±0.06 to 1.5±0.05 mm; mediolateral, 0 to 0.5±0.06 mm; dorsoventral, 2.0±0.07 to 2.9±0.08 mm (all relative to Bregma) and were indistinguishable between experimental groups ($p>0.05$, multiple t-tests on every axis, n=6 each group); the experimenter was blind to the treatment groups while marking the injection sites. For each voxel, the principal fiber orientation was estimated from a structure tensor, which was computed using the image intensity gradients (as a marker of the edges of fiber tracts) within a local neighborhood of the voxel (Bigun and Granlund, 1987; Budde and Annese, 2012; Budde and Frank, 2012; Kass and Witkin, 1987; Khan et al., 2015; Wang et al., 2015). The principal fiber orientation was defined as the tertiary eigenvector (i.e. with the smallest eigenvalue) of the structure tensor. The structure tensor was defined as:

$$S_w(\boldsymbol{p}) = \iiint_{\mathbf{R}^3} w(\boldsymbol{r}) S_0(\boldsymbol{p}-\boldsymbol{r}) d\boldsymbol{r} \quad (1)$$

where $\boldsymbol{p}$ and $\boldsymbol{r}$ represent spatial locations, w is a Gaussian weighing function with standard deviation σ_g, S_0 is a symmetric second-moment matrix derived from image intensity gradients:

$$S_0(\boldsymbol{p}) = \begin{pmatrix} (I_x(\boldsymbol{p}))^2 & I_x(\boldsymbol{p})I_y(\boldsymbol{p}) & I_x(\boldsymbol{p})I_z(\boldsymbol{p}) \\ I_y(\boldsymbol{p})I_x(\boldsymbol{p}) & (I_y(\boldsymbol{p}))^2 & I_y(\boldsymbol{p})I_z(\boldsymbol{p}) \\ I_z(\boldsymbol{p})I_x(\boldsymbol{p}) & I_z(\boldsymbol{p})I_y(\boldsymbol{p}) & (I_z(\boldsymbol{p}))^2 \end{pmatrix} \quad (2)$$

where I_x, I_y and I_z are the gradients of image intensity I along each of the x, y and z axes, computed by convolving I with three 3-dimensional 1st order derivative of Gaussian functions of standard deviation σ_{dog} (Canny, 1986). Structure tensors were computed using MATLAB software (MathWorks, Inc.). Tractography and tractography visualization were performed using Diffusion Toolkit and TrackVis softwares (http://trackvis.org/) respectively.

Cell culture and *in vitro* activity testing

Primary cultured hippocampal neurons were prepared from P0 Sprague-Dawley rat pups and grown on glass coverslips as previously described(Gradinaru et al., 2010). At 12 div cultures were transfected with 1 μg fosCh DNA using calcium phosphate. Immediately following the transfection procedure, cultures were returned to Neurobasal-A culture media (Invitrogen Carlsbad, CA) containing 1.25% FBS (Hyclone, Logan, UT), 4% B-27 supplement (GIBCO, Grand Island, NY), 2 mM Glutamax (GIBCO), and FUDR (2 mg/ml, Sigma, St. Louis, MO) to maintain high basal levels of intrinsic synaptic activity, or they were incubated in unsupplemented Neurobasal media that contained 1 μM tetrodotoxin (TTX), 25 μM 2-amino-5-phosphonopentanoic acid (APV) and 10 μM 2,3-dihydroxy-6-nitro-7-sulfamoyl-benzo[f]quinoxaline-2,3-dione (NBQX) to silence electrical activity. Cultures were stimulated for 30 min by exchanging the media with 60 mM isotonic KCl solution and then fixed with 4% PFA at indicated time points.

***In vivo* optrode recording**

Simultaneous optical stimulation and extracellular electrical recording were performed in isofluorane-anesthetized mice. Optrodes consisted of a tungsten electrode (1 MΩ; 125 μm outer diameter) glued to an optical fiber (300 μm core diameter, 0.37 N.A.), with the tip of the electrode projecting beyond the fiber by 300-500 mm. The optical fiber was coupled to a 473 nm laser and 5 mW light measured at the fiber tip was delivered at 10Hz (5 ms pulses). Signals were amplified and band-pass filtered (300Hz low cut- off, 10 kHz high cut-off) before digitizing and recording to disk. pClamp 10 and a Digidata 1322A board were used to both collect data and generate light pulses through the fiber. The recorded signal was band pass filtered at 300Hz low/5 kHz high (1800 Microelectrode AC Amplifier).

Stereotaxic guidance was used for precise placement of the optrode, which was lowered through the dorsal-ventral axis of the mPFC by 50 μm increments. The percentage of sites yielding light-evoked action potential firing was determined.

Real-time conditioned place preference

Behavioral experiments were performed 2 weeks after virus injections (1.5 μl) during the animals' dark (active) cycle. For induction of fosCh expression under appetitive or aversive conditions, mice received either i.p. injections of cocaine (15 mg/kg) or underwent 20 random foot shocks (2s, 0.5mA, 2 shocks per minute on average). Mice were exposed to appetitive or aversive training twice a day over 5 consecutive days. Conditioned place preference (CPP) was conducted within 12-16 hours after the last appetitive or aversive training. The CPP apparatus consisted of a rectangular chamber with one side compartment measuring 23 cm x 26 cm with multicolored walls, a central compartment measuring 23 cm x 11 cm with white plexiglass walls, and another side compartment measuring 23 cm x 26 cm with distinctive striped walls. Chamber wallpapers were selected such that mice did not display average baseline bias for a particular chamber, and any mouse with a strong initial preference for a chamber was excluded (more than 5 min difference spent in the side chambers during the baseline test). Automated video tracking software (BiObserve) was used to monitor mouse location over 3 consecutive 20 min blocks to assess place preference behavior before, during and after optogenetic stimulation of the fosCh labeled cells. During the light stimulation block, the laser was automatically triggered upon mouse entry into a pre-designated chamber (fully counterbalanced for side) to deliver 2 sec bursts of 10 Hz light pulses every 5 sec (5 ms pulses at 5 mW) for the duration that the mouse remained in the stimulation side. Data are expressed as fold-change in time spent in the light-paired side relative to the initial baseline preference.

Statistics

Two-way ANOVAs were used to assess how gene expression or behavior was affected by other factors (e.g. neuronal activity, optogenetic manipulations). If a statistically significant effect was observed, post hoc testing with correction for multiple comparisons was performed using Tukey's multiple comparisons test. Unpaired t-tests were used for comparisons between two groups. Two-tailed tests were used throughout with $\alpha = 0.05$. Multiple comparisons were adjusted with the false discovery rate method. The experimenter was blinded to the experimental groups while running behavioral experiments and analyzing images. In all figure legends n refers to biological replicates.

Software

All custom software, including the scripts used for atlas building, registration, and analysis as well as codes for CLARITY-based tractography are freely available at: http://capture-clarity.org. The website also provides detailed protocols, sample images and other CLARITY-related resource for download.

Supplemental Table S1, related to Figure 2

		PFC	NAC	BNST	LH	LHb	PVN	BLA	CEA
Home	**Mean**	728.8	811.8	83.6	203.6	166.8	38.4	259.2	343.6
	SEM	151.6	183.2	26.4	65.1	33.6	10.0	77.2	53.1
Cocaine	**Mean**	1937.2	3042.0	674.4	790.6	519.6	62.6	699.0	525.6
	SEM	269.6	871.7	388.3	437.8	226.6	12.6	123.0	85.7
Shock	**Mean**	1334.0	3671.0	449.6	678.0	1841.6	64.0	1068.0	731.2
	SEM	209.8	837.1	55.6	108.0	433.3	14.1	225.8	179.6

Table S1: Number of TRAP cells in brain regions, before normalization, n=5 in each group.

Supplemental References

Akten, B., Kye, M.J., Hao le, T., Wertz, M.H., Singh, S., Nie, D., Huang, J., Merianda, T.T., Twiss, J.L., Beattie, C.E., *et al.* (2011). Interaction of survival of motor neuron (SMN) and HuD proteins with mRNA cpg15 rescues motor neuron axonal deficits. Proc Natl Acad Sci U S A *108*, 10337-10342.

Bigun, J., and Granlund, G.H. (1987). Optimal Orientation Detection of Linear Symmetry. Proceedings of the IEEE First International Conference on Computer Vision, 433-438.

Budde, M.D., and Annese, J. (2012). Quantification of anisotropy and fiber orientation in human brain histological sections. Frontiers in integrative neuroscience *7*, 3.

Budde, M.D., and Frank, J.A. (2012). Examining brain microstructure using structure tensor analysis of histological sections. NeuroImage *63*, 1-10.

Canny, J. (1986). A computational approach to edge detection. Pattern Analysis and Machine Intelligence, IEEE Transactions on, 679-698.

Gradinaru, V., Zhang, F., Ramakrishnan, C., Mattis, J., Prakash, R., Diester, I., Goshen, I., Thompson, K.R., and Deisseroth, K. (2010). Molecular and cellular approaches for diversifying and extending optogenetics. Cell *141*, 154-165.

Guenthner, C.J., Miyamichi, K., Yang, H.H., Heller, H.C., and Luo, L. (2013). Permanent genetic access to transiently active neurons via TRAP: targeted recombination in active populations. Neuron *78*, 773-784.

Kass, M., and Witkin, A. (1987). Analyzing oriented patterns. Computer vision, graphics, and image processing *37*, 362-385.

Kawashima, T., Kitamura, K., Suzuki, K., Nonaka, M., Kamijo, S., Takemoto-Kimura, S., Kano, M., Okuno, H., Ohki, K., and Bito, H. (2013). Functional labeling of neurons and their projections using the synthetic activity-dependent promoter E-SARE. Nat Methods *10*, 889-895.

Khan, A.R., Cornea, A., Leigland, L.A., Kohama, S.G., Jespersen, S.N., and Kroenke, C.D. (2015). 3D structure tensor analysis of light microscopy data for validating diffusion MRI. NeuroImage *111*, 192-203.

Klein, S., Staring, M., Murphy, K., Viergever, M.A., and Pluim, J.P. (2010). elastix: a toolbox for intensity-based medical image registration. IEEE Trans Med Imaging *29*, 196-205.

Mori, S., Crain, B.J., Chacko, V., and Van Zijl, P. (1999). Three-dimensional tracking of axonal projections in the brain by magnetic resonance imaging. Annals of neurology *45*, 265-269.

Sanz, E., Yang, L., Su, T., Morris, D.R., McKnight, G.S., and Amieux, P.S. (2009). Cell-type-specific isolation of ribosome-associated mRNA from complex tissues. Proc Natl Acad Sci U S A *106*, 13939-13944.

Tainaka, K., Kubota, S.I., Suyama, T.Q., Susaki, E.A., Perrin, D., Ukai-Tadenuma, M., Ukai, H., and Ueda, H.R. (2014). Whole-body imaging with single-cell resolution by tissue decolorization. Cell *159*, 911-924.

Tye, K.M., Prakash, R., Kim, S.Y., Fenno, L.E., Grosenick, L., Zarabi, H., Thompson, K.R., Gradinaru, V., Ramakrishnan, C., and Deisseroth, K. (2011). Amygdala circuitry mediating reversible and bidirectional control of anxiety. Nature *471*, 358-362.

Wang, H., Lenglet, C., and Akkin, T. (2015). Structure tensor analysis of serial optical coherence scanner images for mapping fiber orientations and tractography in the brain. Journal of biomedical optics *20*, 036003.

Ye, L., Kleiner, S., Wu, J., Sah, R., Gupta, R.K., Banks, A.S., Cohen, P., Khandekar, M.J., Bostrom, P., Mepani, R.J., *et al.* (2012). TRPV4 is a regulator of adipose oxidative metabolism, inflammation, and energy homeostasis. Cell *151*, 96-110.